ASEAN Journal of Science and Engineering

Journal homepage: http://ejournal.upi.edu/index.php/AJSE/

Enhanced Hydrogen Production from Biomass Pyrolysis using Surfactant-Modified Na-Bentonite Catalyst

Dwi Irawan[1,2,], Widya Wijayanti[1], Slamet Wahyudi[1], Herma Nugroho Rono Adi Kusumo[1], Ahmad Yani[1], I.N.G. Wardana[1]*

[1]Brawijaya University, Malang, Indonesia
[2]Muhammadiyah Metro University, Lampung, Indonesia
Correspondence: E-mail: irawan.ke10@gmail.com

ABSTRACT

This study investigates the improvement of hydrogen gas production in biomass pyrolysis through the use of Na-bentonite catalysts modified with methyl ester sulfonate (MES), a biodegradable anionic surfactant. Corn cob powder was used as the biomass feedstock in a fixed-bed pyrolysis reactor at 550°C. The MES modification introduced alkyl, ester, and sulfonate functional groups, increasing the catalyst porosity, surface area, and acidity. Structural and chemical changes were confirmed by FTIR, XRD, UV-Vis, SEM, and EDX analyses. The MES-modified Na-bentonite catalyst significantly enhanced hydrogen production, reaching 876 ppm (a 25.11% increase compared to pyrolysis without a catalyst) and also lowered the reaction temperature and shortened the reaction time. Methane production decreased as MES improved catalyst selectivity toward dehydrogenation pathways. The results indicate that MES-modified Na-bentonite is a low-cost, efficient, and environmentally friendly catalyst suitable for improving hydrogen yields in biomass pyrolysis, offering a promising alternative to conventional metal-based catalysts.

ARTICLE INFO

Article History:
Submitted/Received 05 May 2025
First Revised 02 Jun 2025
Accepted 06 Aug 2025
First Available online 07 Aug 2025
Publication Date 01 Dec 2025

Keyword:
Biomass,
Catalyst,
Hydrogen,
Methane,
Pyrolysis.

1. INTRODUCTION

The energy demand continues to rise with the growth of society and industry across the globe. As a result, the reliance on fossil fuels is decreasing due to their limited availability and the significant CO_2 emissions that negatively impact environmental quality [1, 2]. In response, the development of biomass-based renewable energy is on the rise, as it is abundant and considered a carbon-neutral fuel that can help mitigate environmental issue [3, 4]. In addition, the use of sustainable biomass reduces agricultural, forestry, and other organic waste. One product of biomass utilization as renewable energy is hydrogen fuel, produced using the thermochemical method of pyrolysis/gasification [5].

The thermochemical process of biomass pyrolysis breaks down carbon-rich feedstock to produce gaseous products, with little or no oxygen. This mechanism produces syngas. They are rich in hydrogen, carbon monoxide, methane, ethylene, propylene, butane, and other hydrocarbons [6, 7]. The pyrolysis mechanism involves the chemical decomposition of biomass through heating, with minimal or no oxygen present. Several strategies have been employed to enhance hydrogen gas production, including the use of catalysts [8]. Catalysts are crucial in increasing the selectivity for hydrogen production while reducing activation energy [9]. They facilitate the breakdown of heavier hydrocarbon compounds in volatiles into lighter hydrocarbons, including hydrogen, through cracking and steam reforming reactions [10]. Various types of catalysts are commonly used, including metal and non-metal catalysts [11]. Metal catalysts can increase the concentration of hydrogen in syngas [12]. For instance, some researchers [13] stated that Nickel-based catalysts have shown potential in enhancing hydrogen production during the pyrolysis process, indicating their effectiveness in improving overall production efficiency. While metal catalysts are valued for their good oxygen mobility and redox properties, they have limitations, such as low diffusion, which can affect the adsorption and desorption of reactants at the active site. Additionally, issues like metal deposition and sintering can arise [14]. Metal catalysts are also typically more expensive and may generate waste that poses a risk of environmental pollution [15].

One of the non-metal catalysts that has been widely studied and shows significant potential is bentonite. Bentonite is a clay mineral rock characterized by high porosity, mechanical and thermal stability, a large specific surface area, and remarkable ion exchange capacity [16]. The basic structure of bentonite consists of a phyllosilicate layer, which contains tetrahedral silicon-oxygen sheets and octahedral aluminum-oxygen-hydroxide sheets [17]. Bentonite's silicate layer carries a negative charge and features easily exchangeable cations, notably calcium (Ca^{2+}) and sodium (Na^{+}), leading to the classification of bentonite into two types: calcium bentonite (Ca-bentonite) and sodium bentonite (Na-bentonite). Na-bentonite with sodium content that can be exchanged with other compounds (cation exchange), and can expand (swell) when in contact with water. Na-bentonite with cation exchange ability allows modification with other compounds [18], enabling it to be modified by intercalating or inserting other compounds such as polymers, metal ions, surfactants, or organic compounds into the Na-bentonite silicate layer [19]. Surfactants have hydrophilic and hydrophobic groups that will help change the surface structure of Na-bentonite to hydrophobic and increase the surface area and adsorption capacity for organic molecules [20]. This study uses anionic surfactants because of their biodegradable and environmentally friendly properties. The anionic surfactant used in this study is Methyl Ester Sulfonate (MES).

MES is an anionic surfactant produced through the sulfonation process of fatty acid methyl esters derived from vegetable oils. Thus, it is more environmentally friendly, sustainable, and cost-effective [21]. It has a long and hydrophobic carbon chain (C12-C18), which can interact

DOI: https://doi.org/10.17509/ajse.v5i3.88898
p- ISSN 2776-6098 e- ISSN 2776-5938

with the Na-bentonite layer, replacing Na+ ions on its surface and changing the hydrophilic properties of Na-bentonite to be more hydrophobic. MES will help open the pores of Na-bentonite to create a more porous structure [22], increase the surface area [21], increase the basal distance of bentonite [23], crystallinity [24], hydrophobicity [23], so that it will affect the activity and selectivity of bentonite as a catalyst to increase hydrogen production in the biomass pyrolysis process [25]. Modification of bentonite using surfactants has been widely studied [26-29].

This study introduces the novel use of Na-bentonite modified with Methyl Ester Sulfonate (MES), a biodegradable anionic surfactant, as an environmentally friendly catalyst to enhance hydrogen and methane production in biomass pyrolysis. While various studies have explored surfactant-modified bentonites, no previous work has specifically examined the structural characteristics, catalytic activity, and reaction kinetics of MES-modified Na-bentonite in this context. The long carbon chain and sulfonate group of MES contribute to increasing acid sites, improving porosity and hydrophobicity, and facilitating the dehydrogenation pathway toward light gas formation such as H_2. Therefore, this study offers a cost-effective, sustainable alternative to metal-based catalysts, with significant potential to advance green energy conversion technologies.

2. METHODS

2.1. Material Characteristics

The biomass material used in this research was corn cob powder. The chemical composition of corn cobs is presented in **Table 1** [30]. The corn cob powder was dried in an oven at 150°C for 1 hour until the moisture content reached 9%. Dried corn cob powder was sieved to even out the size using 40 sieve. The catalyst employed in this study was Na-bentonite, with the following chemical composition: SiO_2 61.4%, Al_2O_3 19.8%, Fe_2O_3 3.9%, Na_2O 2.2%, K_2O 0.4%, CaO 0.6%, MgO 1.3%, and H_2O 7.2%. This study utilized an anionic surfactant, namely MES, which was modified on Na-bentonite to produce a Na-bentonite + MES catalyst.

The mechanism of Na-bentonite catalyst modification was carried out and presented in **Figure 1**, namely 50 g of MES dissolved in 500 mL of Aquades into a glass flask using a magnetic stirrer at a temperature of 80 0C, rpm 300, stirred for 10 minutes. Then, 50 g of Na-bentonite was slowly inserted into the glass flask and continued to stir for 120 minutes. The mixture of Na-bentonite and MES was cooled and washed with Aquades to remove any excess MES. After washing, the sample was dried for 120 minutes in an oven at a temperature of 100°C, then ground to a mesh size of 400 using a mortar.

Catalyst samples, both Na-bentonite and Na-bentonite + MES, were tested to analyze the characteristics of the catalyst to assess any changes in their physical and surface properties following modification. Several tests were employed, namely: (i) Fourier Transform Infrared Spectroscopy (FTIR) testing, performed using an IRSpirit-T spectrometer (Shimadzu, Japan), was used to characterize the materials and measure the chemical composition or functional groups present in the catalyst. FTIR operates by measuring the absorbance of infrared light by the catalyst, producing a spectrum that reflects the strain vibrations in the sample; (ii) X-ray diffraction (XRD) testing is a non-destructive analysis technique to analyze the crystalline phase and basal distance of Na-bentonite and Na-bentonite + MES catalysts. XRD testing uses PANalytical X'Pert PRO. XRD determines the lattice structure and particle size, determining the crystallinity of the catalyst samples [31]; (iii) UV-Vis spectrophotometer testing measured the absorbance of catalyst particles using UV light wavelengths (200–400 nm) and visible light (400–1000 nm) with the results of absorbance, transmittance, or scan wavelength values; (iv) Scanning Electron Microscope (SEM) and Energy Dispersive x-ray spectroscopy (EDX) testing

DOI: https://doi.org/10.17509/ajse.v5i3.88898
p- ISSN 2775-6793 e- ISSN 2775-6815

using Inspect S50 FEI. SEM-EDX testing was used to evaluate the morphology and topography of the sample surfaces and to determine the chemical element composition of the Na-bentonite and Na-bentonite + MES catalyst samples.

Table 1. Chemical properties of corn cob powder.

Chemical Properties	
Ash content	1,33%
Lignin	35,2%
Cellulose	41,5%
Hemicellulose	13,0%
Others	8,97%

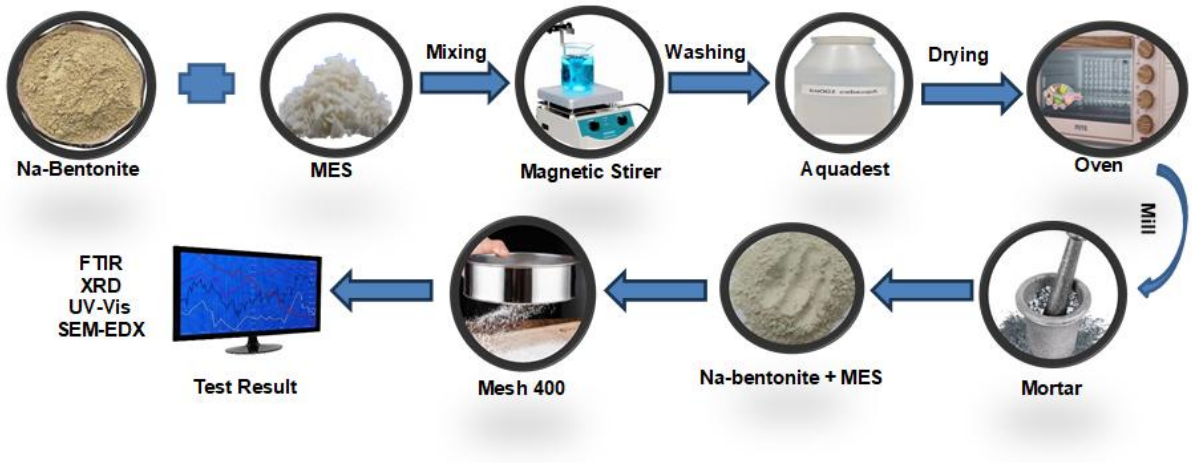

Figure 1. Bentonite preparation procedure.

2.2. Pyrolysis Experiment Setup

Pyrolysis testing was conducted using the experimental equipment illustrated in **Figure 2**. Pyrolysis testing used a cylindrical tube reactor made of stainless steel with a diameter of 8 inches and a height of 5 inches (1). Raw materials of 100 g of corn cob powder were placed into the reactor (2). The reactor was heated using LPG fuel (3) and a heating stove (4). This pyrolysis setup utilized an ex-situ system with a catalyst placed on the top of the reactor (5), allowing the volatile gases to pass through the catalyst. The reactor flowed with inert gas using nitrogen with a flow rate of 1000 mL/minute for 10 minutes to create an inert atmosphere (6), the heating process continued until the reactor reached a temperature of 550°C, the temperature of 550°C is used because it can reduce the formation of tar and semi-coke by optimizing the biomass decomposition process. Using a temperature below that will produce more tar, while utilizing a temperature too high will produce unreactive charcoal and reduce hydrogen production. Other studies revealed that pyrolysis at a temperature of 550°C is more efficient in producing hydrogen [32, 33]. Volatile gas was flowed through a 10 mm diameter stainless steel pipe (7), into a spiral heat exchanger pipe to reduce the gas temperature (8). The gas, after cooling, was directed into a tube containing ice to condense the water vapor (9). The temperature during pyrolysis was observed using a K-type thermocouple (10) placed inside the reactor. The gas product from pyrolysis was measured for methane and hydrogen gas content using MQ-4 and MQ-8 sensors after being calibrated (11). All sensors were channeled to the Arduino Uno (12) as an interface to obtain temperature data, methane, and hydrogen content, the results of which were in the computer (13). The test was repeated at

DOI: https://doi.org/10.17509/ajse.v5i3.88898
p- ISSN 2776-6098 e- ISSN 2776-5938

the same room temperature using variations without catalyst, Na-bentonite catalyst, and Na-bentonite + MES.

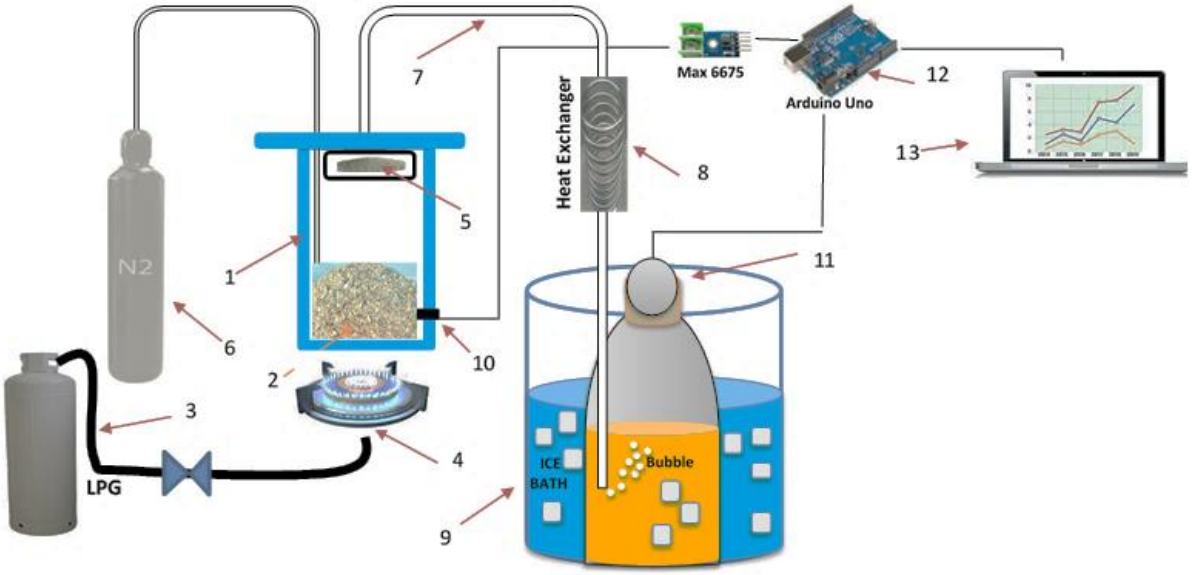

Figure 2. Research scheme.

3. RESULTS AND DISCUSSION

3.1. Functional Group Analysis

Changes in the functional groups of Na-bentonite and Na-bentonite + MES were evaluated based on the FTIR spectra presented in **Figure 3**. The FTIR spectrum of Na-bentonite contained a band of 3624 cm^{-1}, indicating the stretching vibration of O-H bound to Al^{3+} or Mg^{2+} [34], at bands 3405 and 1633 cm^{-1} from the stretching vibration of H-O-H from adsorbed water [35]. The main bands at 1116, 998, 795, and 678 cm^{-1} were caused by the stretching vibration of Si-O [36], the peak of 912 cm^{-1} was caused by the deformation of AL-AL-OH, and the peak of 518 cm^{-1} was caused by the deformation of AL-O-Si [37]. In the FTIR spectrum of Na-bentonite + MES, there were new absorption bands of 2918 and 2849 cm^{-1}. They showed the aliphatic C-H stretching vibration of the methylene group (-CH_2-) and the methyl group (-CH_3), indicating the presence of aliphatic hydrocarbon chains caused by the hydrocarbon tail of the surfactant [38, 39]. This change in the surface properties of the Na-bentonite catalyst indicated a shift from being hydrophilic to hydrophobic, which facilitated the adsorption of non-polar organic molecules during the cleavage of C-H bonds [40]. Furthermore, a new absorption peak was observed at 1724 cm^{-1}, indicating the stretching (C=O) of the ester in the compound containing the carbonyl group of the MES molecule. Na-bentonite modified with MES could cause changes in the interlayer distance of bentonite and increased porosity and surface area, all of which could contribute to increased catalytic activity [41]. Spectral peaks were 1420 cm^{-1}, 1208 cm^{-1}, and 1116 cm^{-1}. The increase in intensity of these bands could be attributed to the S=O stretching of the sulfonate group. This group's presence identified the presence of acid sites on Na-bentonite + MES [42]. These sulfonate groups provided Bronsted acid sites, which could attract protons (H^+) from organic molecules, helping to facilitate the cleavage of C-H bonds and producing hydrogen (H_2) during the pyrolysis process [43], the 720 cm^{-1} band indicated the presence of Si-C_6H_5 groups [24] and the 620 cm^{-1} band indicated Al-O and Si-O groups [44], from several new appearing absorptions indicating the success of MES modification on Na-bentonite and changing the chemical properties of the bentonite surface,

DOI: https://doi.org/10.17509/ajse.v5i3.88898
p- ISSN 2775-6793 e- ISSN 2775-6815

providing hydrophobic functionality that increased its interaction with non-polar hydrocarbon molecules [45].

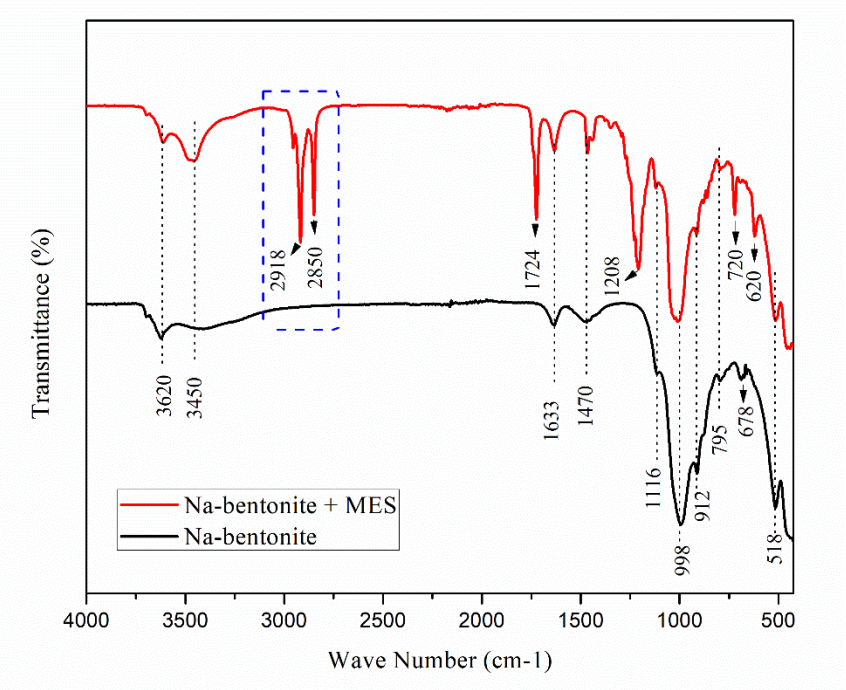

Figure 3. FTIR test results.

3.2. Crystal Structure Analysis

The XRD pattern of the catalyst sample was analyzed and presented in **Figure 4**. The results for Na-bentonite showed a d001 value with a basal spacing of 4.48 Å, appearing at an angle of 19.81°. In contrast, the Na-bentonite combined with MES displayed a main peak shifted to around 14.79° with a plane distance (d001) of 5.98 Å, indicating an increase in basal spacing. This increase identified that MES successfully entered into the Na-bentonite layer structure, with the rearrangement of atoms in the crystal structure increasing the crystallinity of Na-bentonite + MES [46]. The increase in crystallinity will increase the accessibility of the active site of the Na-bentonite + MES catalyst, which will contribute to the efficiency of chemical reactions and increase the adsorption capacity of organic compounds during the pyrolysis of corncob powder biomass [47]. The increase in basal spacing and crystallinity of Na-bentonite + MES will improve the catalytic performance and thermal stability of the catalyst in an effort to increase hydrogen production in the catalytic pyrolysis of biomass [48].

DOI: https://doi.org/10.17509/ajse.v5i3.88898
p- ISSN 2776-6098 e- ISSN 2776-5938

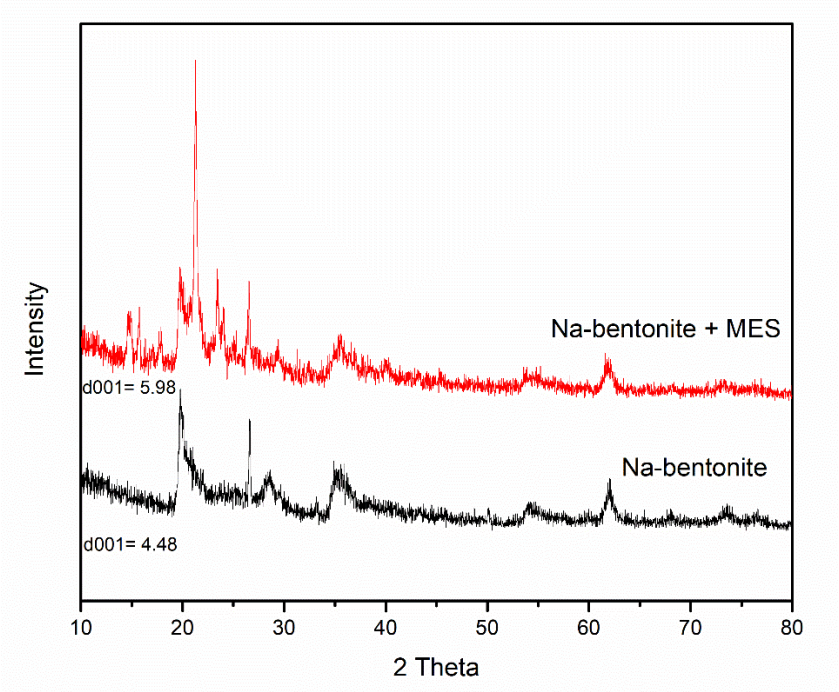

Figure 4. XRD test results.

3.3. Absorbance Analysis

The results of the UV-Vis characteristic test of Na-bentonite and Na-bentonite + MES catalysts are presented in **Figure 5**. The test shows two absorbance peaks from both samples, Na-bentonite at 260 and 352 nm, and Na-bentonite + MES at 286 and 392 nm. The absorption of 260 nm indicates the presence of electronic transitions originating from the structure of the Na-bentonite layer containing organic groups on the surface of the Na-bentonite catalyst. The absorbance peak at 352 nm indicates the presence of a π-π* transition related to the Al metal content adsorbed on the Na-bentonite layer. The absorbance peak at 286 nm indicates a change or increase in the absorbance of Na-bentonite + MES due to changes in the energy of the π-π* transition originating from the alkyl and ester groups. This shows the transfer of electrons from the Highest Occupied Molecular Orbital (HOMO) of the alkyl group to the Lowest Unoccupied Molecular Orbital (LUMO) [49]. The absorbance peak at 392 nm is associated with the n-π* transition of the free atom of the sulfonate group, affecting the HOMO and LUMO distances with a smaller energy [50]. The results of the modification of Na-bentonite using MES show changes in the HOMO and LUMO transition energies, shown in the new peaks of 286 and 392 nm, with the addition of alkyl, ester, and sulfonate groups increasing catalytic activity [51, 52]. The HOMO and LUMO energy gaps that occur between Na-bentonite and Na-bentonite + MES are 4.77 and 4.34 eV. This shows a decrease in the energy gap after modification, which increases the accessibility of the active site of the catalyst and improves catalytic performance [53].

DOI: https://doi.org/10.17509/ajse.v5i3.88898
p- ISSN 2775-6793 e- ISSN 2775-6815

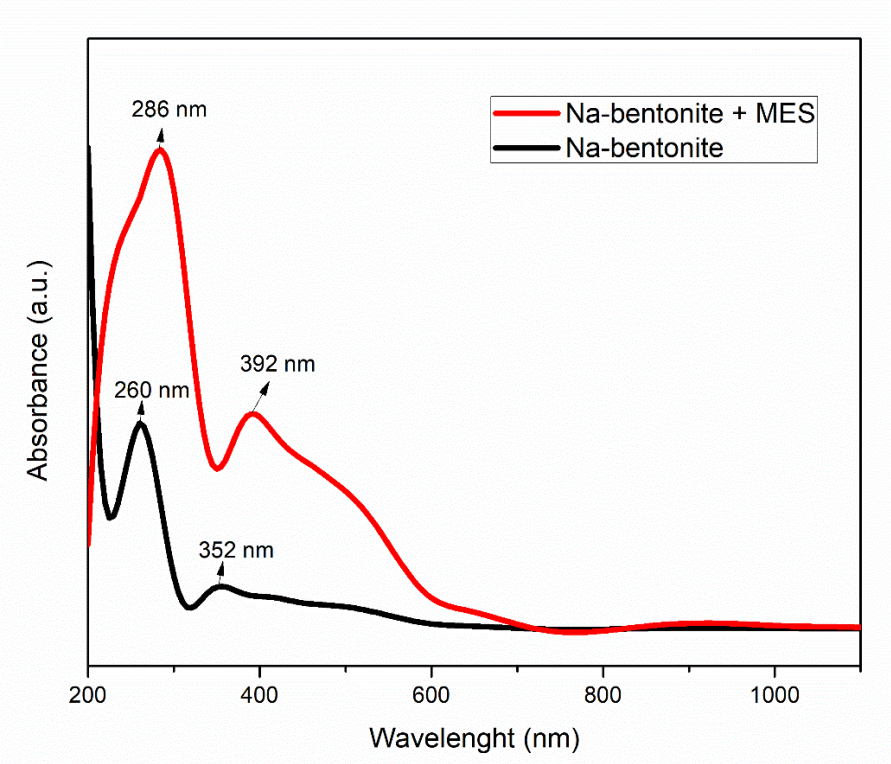

Figure 5. UV-Vis test results.

3.4. Surface Morphology Analysis

The results of the SEM testing are illustrated in **Figure 6**. The characteristics of the Na-bentonite catalyst are shown in **Figure 6(a)**, which reveals a solid, stacked particle structure with a rough surface. This roughness can reduce the catalyst's contact area and its adsorption capacity for organic compounds [54]. The surface charge of the catalyst was analyzed using image software, which determines the type of charge based on the brightness or intensity of the images [55, 56]. **Figure 6(b)** displays a dark and uneven contour color, indicating that the Na-bentonite catalyst carries a negative charge. This negative charge likely arises from the presence of negatively charged sites from the silicate (SiO_4) and alumina (AlO_4) groups within the Na-bentonite structure [57].

The surface morphology of Na-bentonite + MES is shown in **Figure 6(c)**, also at a magnification of 10,000x. In this case, the morphological structure is more dispersed, with open layers that create larger pores and an increased surface area. These observations are consistent with the XRD results, which indicate an increase in the basal spacing distance in the Na-bentonite + MES layers. **Figure 6(d)** illustrates the charge distribution of Na-bentonite + MES, showing a brighter and more uniform colour distribution. Colours such as yellow and red indicate that Na-bentonite + MES has a positive charge. This positive charge is attributed to the sulfonate groups from MES, which enhance Bronsted acid sites, as well as the long alkyl chains that increase electron interactions on the surface. This improvement in surface properties also results in greater light absorption, as evidenced by the formation of new peaks in the UV-Vis spectrum [58].

DOI: https://doi.org/10.17509/ajse.v5i3.88898
p- ISSN 2776-6098 e- ISSN 2776-5938

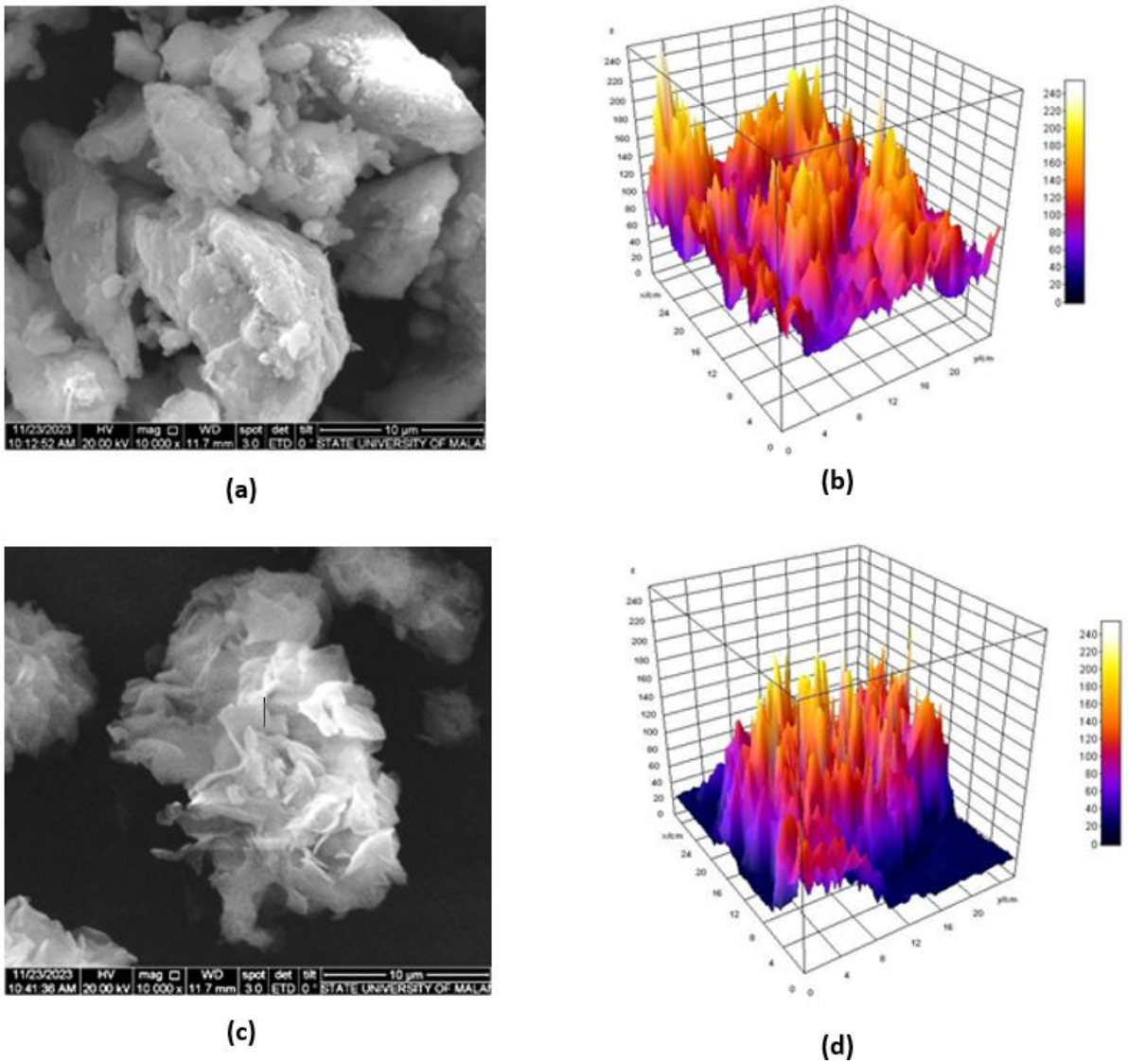

Figure 6. SEM and surface images of Na-bentonite (a, b), Na-bentonite + MES (c, d).

3.5. Material Composition Analysis

Following the morphological structure testing with SEM, we performed EDX testing to assess the distribution and composition of Na-bentonite and Na-bentonite modified with MES. **Figure 7(a)** displays the elemental composition of Na-bentonite, which consists of 21.2% carbon (C), 47.1% oxygen (O), 0.9% sodium (Na), 0.7% magnesium (Mg), 6.3% aluminum (Al), 9.6% silicon (Si), 1.4% calcium (Ca), 0.3% titanium (Ti), and 12.5% iron (Fe). The high concentrations of silicon and aluminum indicate that the structure of Na-bentonite is primarily made up of silicate and alumina sheets, forming the main framework of the material.

Figure 7(b) presents the elemental composition of Na-bentonite + MES, consisting of 57.7% carbon (C), 29.5% oxygen (O), 3.3% sodium (Na), 0.2% magnesium (Mg), 1.9% aluminum (Al), 3.4% silicon (Si), 2.9% sulfur (S), 0.3% calcium (Ca), and 0.9% iron (Fe). **Figure 7(b)** shows the composition of Na-bentonite + MES elements consisting of 57.7% C, 29.5% O, 3.3% Na, 0.2% Mg, 1.9% Al, 3.4% Si, 2.9% S, 0.3% Ca, and 0.9% Fe. The long alkyl chain of MES shows success in changing the chemical composition of the catalyst, as seen in the increase in carbon value from 21.2% to 57.7%, which indicates that Na-bentonite + MES becomes hydrophobic. In addition to the increase in carbon elements, there is the addition of new elements from the sulfonate group, with a sulfur (S) content reaching 2.9%. The success of the modification is

DOI: https://doi.org/10.17509/ajse.v5i3.88898
p- ISSN 2775-6793 e- ISSN 2775-6815

also shown by the decrease in Silica and Alumina elements, which facilitate the adsorption of organic compounds and the performance of the Na-bentonite + MES catalyst.

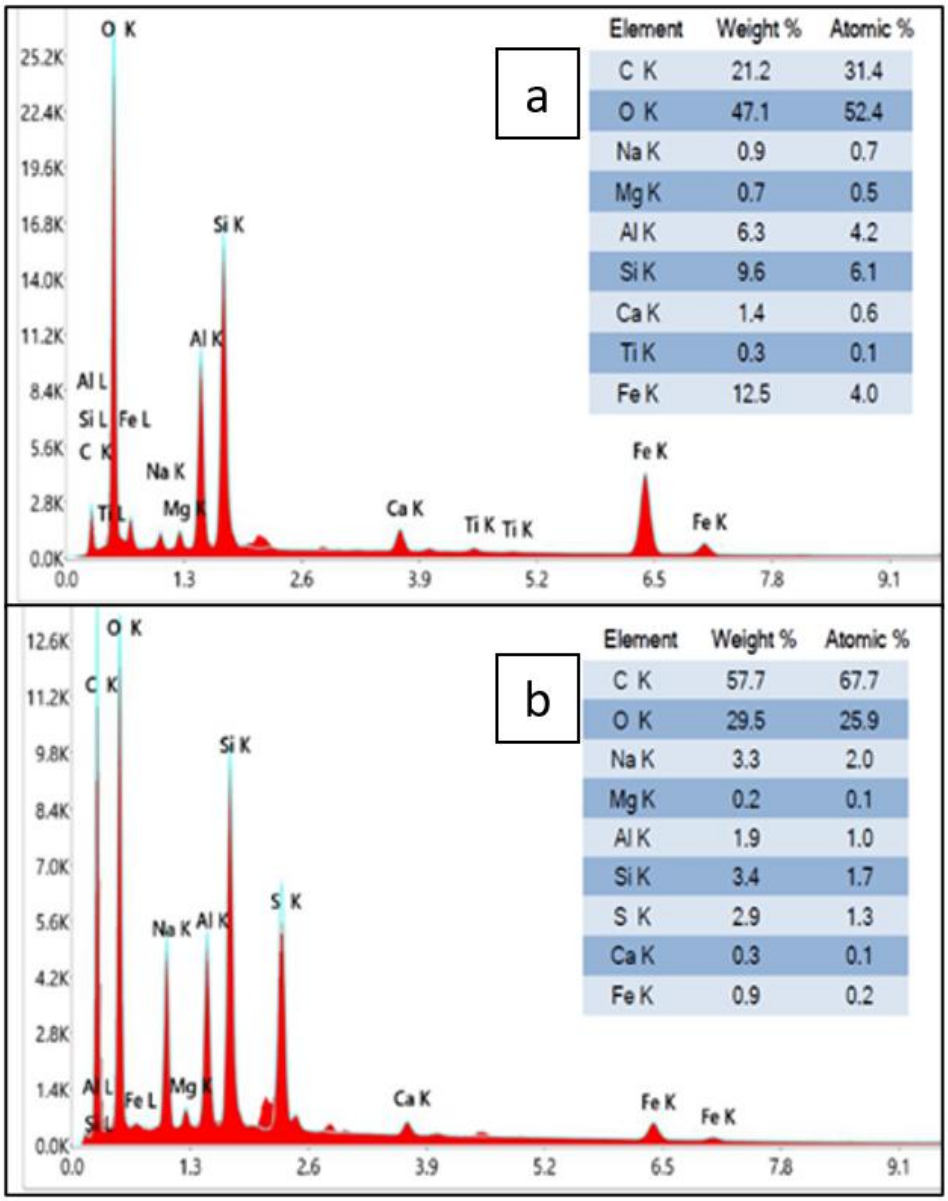

Figure 7. Na-bentonite (a) and Na-bentonite + MES composition data (b).

3.6. The Role of Catalysts in Methane and Hydrogen Production at Different Reaction Temperatures

Figure 8 illustrates the production of methane and hydrogen during biomass pyrolysis with and without catalysts, specifically Na-bentonite and Na-bentonite combined with MES. Methane production data are shown in **Figure 8(a)**. Without a catalyst, methane production was slow, peaking at 442 ppm at a temperature of 424°C. In contrast, the Na-bentonite catalyst achieved a peak of 569 ppm, while the Na-bentonite + MES combination was reaching MES 497 ppm. The Na-bentonite catalyst provided active sites that accelerated the breakdown of organic molecules, which enhanced the cleavage of C-H bonds [59], significantly increasing the methane production rate by 22.31%. Na-bentonite + MES has a sulfonic acid site that increases the selectivity of the catalyst to the dehydrogenation reaction, which reduces methane formation and increases hydrogen formation [60]. As depicted in **Figure**

DOI: https://doi.org/10.17509/ajse.v5i3.88898
p- ISSN 2776-6098 e- ISSN 2776-5938

8(b), hydrogen production remains more consistent across all temperature ranges. The highest hydrogen production occurred at 500°C, reaching 876 ppm, compared to 842 ppm with Na-bentonite and 656 ppm without any catalyst. The use of the Na-bentonite + MES catalyst could enhance hydrogen production by 25.11% compared to the non-catalytic process, demonstrating that this catalyst selectively promoted hydrogen gas production. Additionally, the Na-bentonite + MES catalyst accelerated the reaction at a temperature of 308°C, while Na-bentonite alone required a temperature of 321°C. The sulfur content in Na-bentonite + MES, which added Bronsted acid sites, significantly contributed to increasing catalytic activity by providing more active sites for dehydrogenation reactions [61]. **Figure 8(c)** presents methane production at a temperature of 300-550°C. The Na-bentonite and Na-bentonite + MES catalysts produced the highest methane at 450°C, but at high temperatures of 500-550°C methane production decreased significantly, especially in Na-bentonite + MES. This indicates that Na-bentonite is more selective towards methane formation, while Na-bentonite + MES directs the reaction more towards dehydrogenation, reducing CH_4 production at high temperatures [62].

The molecular reaction mechanism of Methyl ester sulfonate (MES) and radical molecules during the pyrolysis process is shown in **Figure 9**. MES with a sulfonate group had a significant role in donating protons (H^+) and triggering the formation of free radicals, which accelerated dehydrogenation reactions in organic molecules [63]. This dehydrogenation reaction was strengthened by the presence of Bronsted acid sites, which accelerated the breakdown of chemical bonds and sped up the pyrolysis reaction. The formation of hydroxyl radicals (*OH) from the interaction of hydroxyl groups in water (H_2O) facilitated the cleavage of C-H bonds in organic compounds such as methane (CH_4), producing carbon radicals [64]. At high temperatures, methane (CH_4), carbon monoxide (CO), and water (H_2O) were released. MES helped break C-H bonds, producing hydrogen gas (H_2) through cleavage of protons (H^+), and hydroxyl radicals helped further oxidation of CO and CH_4 to carbon dioxide (CO_2) and hydrogen (H_2) [65].

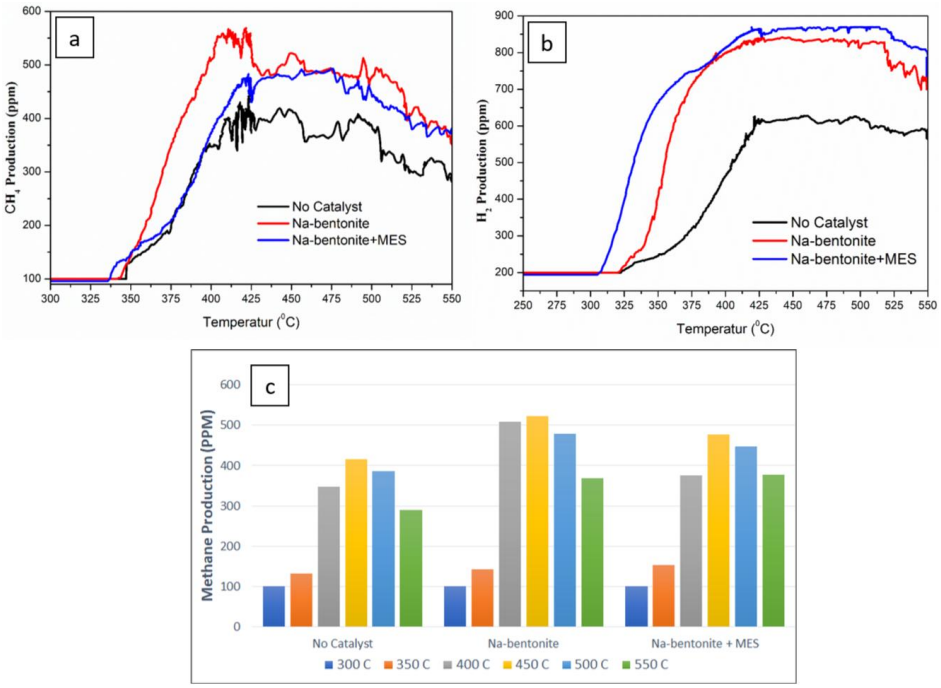

Figure 8. Effect of Na-bentonite and Na-bentonite + MES on methane and hydrogen production. (a). Methane production (b). Hydrogen production (c). Effect of temperature on methane production.

DOI: https://doi.org/10.17509/ajse.v5i3.88898
p- ISSN 2775-6793 e- ISSN 2775-6815

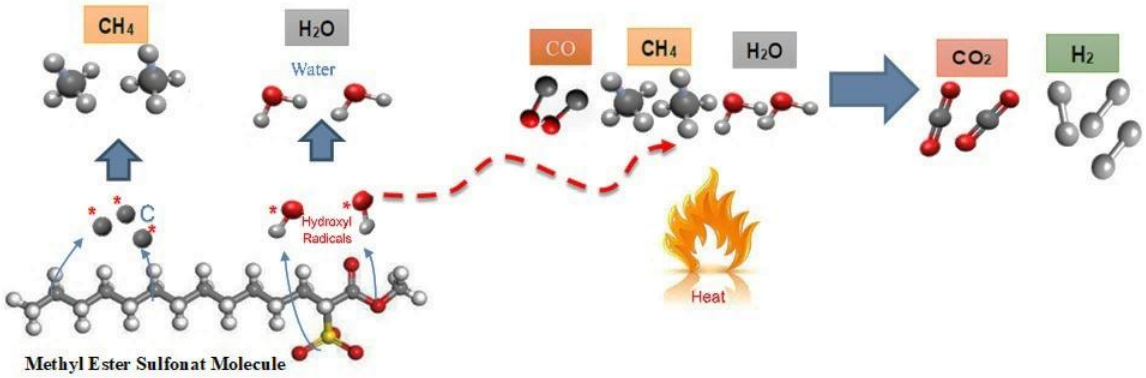

Figure 9. The MES reaction mechanism accelerated hydrogen production.

3.7. Methane and Hydrogen Production Over Time

Figure 10 presents the production of methane and hydrogen regarding the duration of the pyrolysis tests. The use of catalysts significantly influences the production of both gases, affecting not only the reaction temperature but also the time needed to generate hydrogen gas. In **Figure 10(a)**, hydrogen production is shown at the gas formation temperature. Higher temperatures resulted in increased hydrogen production. When using Na-bentonite combined with MES catalysts, hydrogen production remained high at a temperature of 500°C, while other catalysts began to decline. These findings suggested that catalysts with greater surface area and porosity enhanced catalytic efficiency. The XRD test results (shown in **Figure 4**) indicated that Na-bentonite combined with MES had a larger porosity and basal spacing, facilitating better adsorption of organic molecules at elevated temperatures. **Figure 10(b)** illustrates methane production, with Na-bentonite yielding significantly higher methane gas output. It demonstrated that Na-bentonite is very effective in accelerating pyrolysis and methane formation at high temperatures. However, at temperatures exceeding 500°C, methane production started to decline, suggesting that dehydrogenation reactions began to dominate. Na-bentonite exhibited superior adsorption capacity and active sites that accelerated the pyrolysis process. XRD (**Figure 4**) and SEM (**Figure 6**) analyses confirmed that Na-bentonite has a layered structure and good porosity, which allowed for more effective interactions between organic molecules and the catalyst's surface. Notably, Na-bentonite is more selective in methane gas formation compared to hydrogen gas, as evidenced by lower hydrogen production compared to the Na-bentonite + MES catalyst. In **Figure 10(c)**, hydrogen production reached 876 ppm, representing an increase of 25.11%. The reaction times for hydrogen gas formation showed a significant difference. The formation of hydrogen gas using the Na-bentonite + MES catalyst began at 68 seconds, while the Na-bentonite catalyst started at 113 seconds. The sulfonate group resulting from the modification with MES provided Brønsted acid sites that facilitated the cleavage of C-H and C-C bonds in organic molecules [32]. The presence of sulfonate groups was supported by the FTIR test results in **Figure 3**, and the increase in sulfur content was confirmed by the EDX results in **Figure 7**, indicating an enhancement in catalytic activity for hydrogen gas production.

Figure 11 shows the success of Na-bentonite catalyst modification using MES in producing methane and hydrogen-rich gas. MES has a long-chain alkyl group, changing hydrophilic Na-bentonite to hydrophobic and increasing carbon content, thereby increasing the number of active sites that can break O-H and C-H bonds. The resulting ester group increases the thermal stability of the catalyst in maintaining degradation at high temperatures in **Figure 10(a)**.

DOI: https://doi.org/10.17509/ajse.v5i3.88898
p- ISSN 2776-6098 e- ISSN 2776-5938

Hydrogen production was still high at a temperature of 500°C. The sulfonate group increased the acidic properties to help release H^+ protons from organic compounds and form hydrogen gas (H_2) [66, 67]. As shown in **Figure 10(a)**, hydrogen gas production continued to increase even at 500°C [68]. The sulfonic group contributed by providing Bronsted acid sites, which helped in breaking down C-H bonds by withdrawing electrons, thereby making it easier to separate these bonds into protons (H^+) [63]. While Na-bentonite is effective in facilitating pyrolysis reactions at medium temperatures, its selectivity decreases at high temperatures, resulting in reduced methane production. This decreased production may occur because the reaction shifts from breaking C-H bonds to favoring dehydrogenation reactions, which are more dominant at elevated temperatures. The mechanism for breaking the C-H bond occurred when hydrocarbons interacted with Brønsted and Lewis acids. This interaction increased the polarity of the C-H bond, weakening it and leading to a dehydrogenation reaction that produced carbon monoxide (CO) and hydrogen (H_2) [69].

Overall, pyrolysis using corn cob powder biomass can generate methane and hydrogen. The addition of catalysts can enhance this production. For example, using a Na-bentonite catalyst increased methane production by 22.32%, while hydrogen production increased by 22%. However, when the Na-bentonite catalyst was modified with mesoporous silica (MES), methane production decreased to 11%, but hydrogen production rose to 25.11%. The reduction in methane production was due to the Na-bentonite + MES catalyst's ability to convert CH_4 to H_2 through the dehydrogenation process during pyrolysis [70]. Additionally, the Na-bentonite + MES catalyst accelerated the pyrolysis reaction time from 115 seconds to 68 seconds and lowered the reaction temperature from 321 to 308°C. This catalyst is a viable option because it is environmentally friendly, thus minimizing the risks of environmental damage, and it is cost-effective due to its low price.

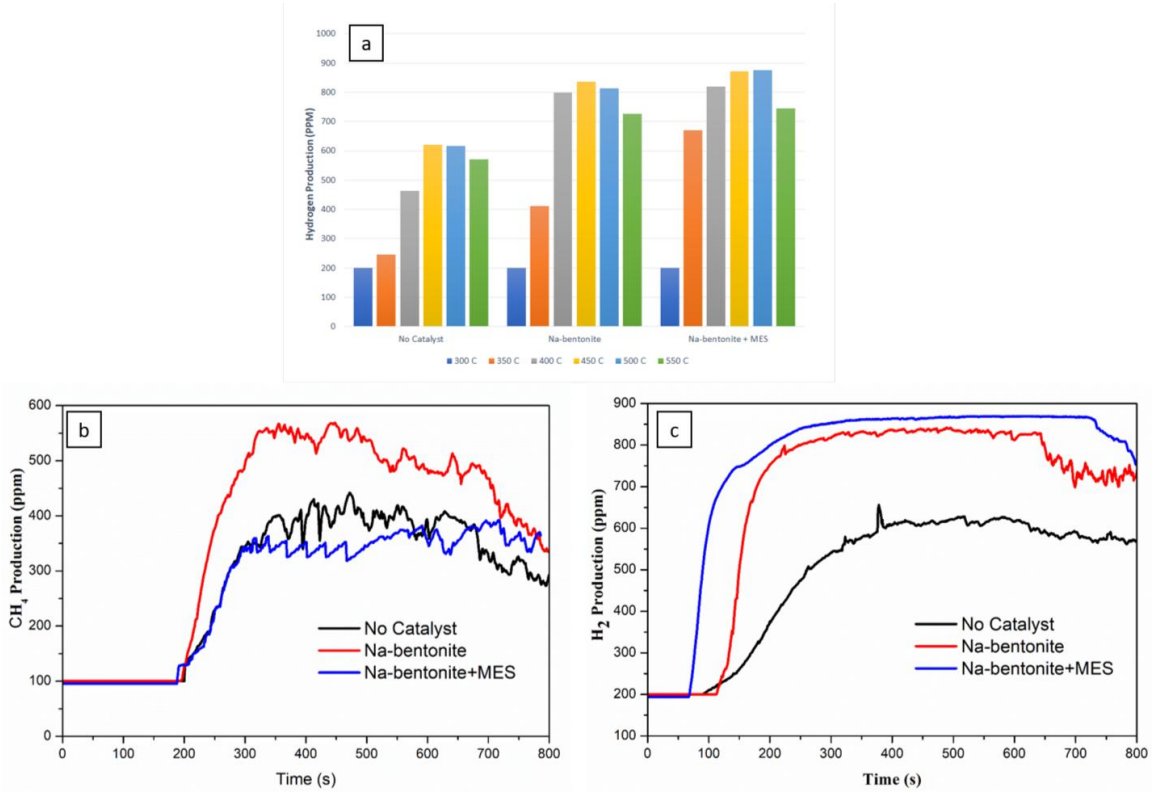

Figure 10. Effects of catalyst on methane and hydrogen production: (a) influence of temperature on hydrogen production; (b) methane production; (c) hydrogen production.

DOI: https://doi.org/10.17509/ajse.v5i3.88898
p- ISSN 2775-6793 e- ISSN 2775-6815

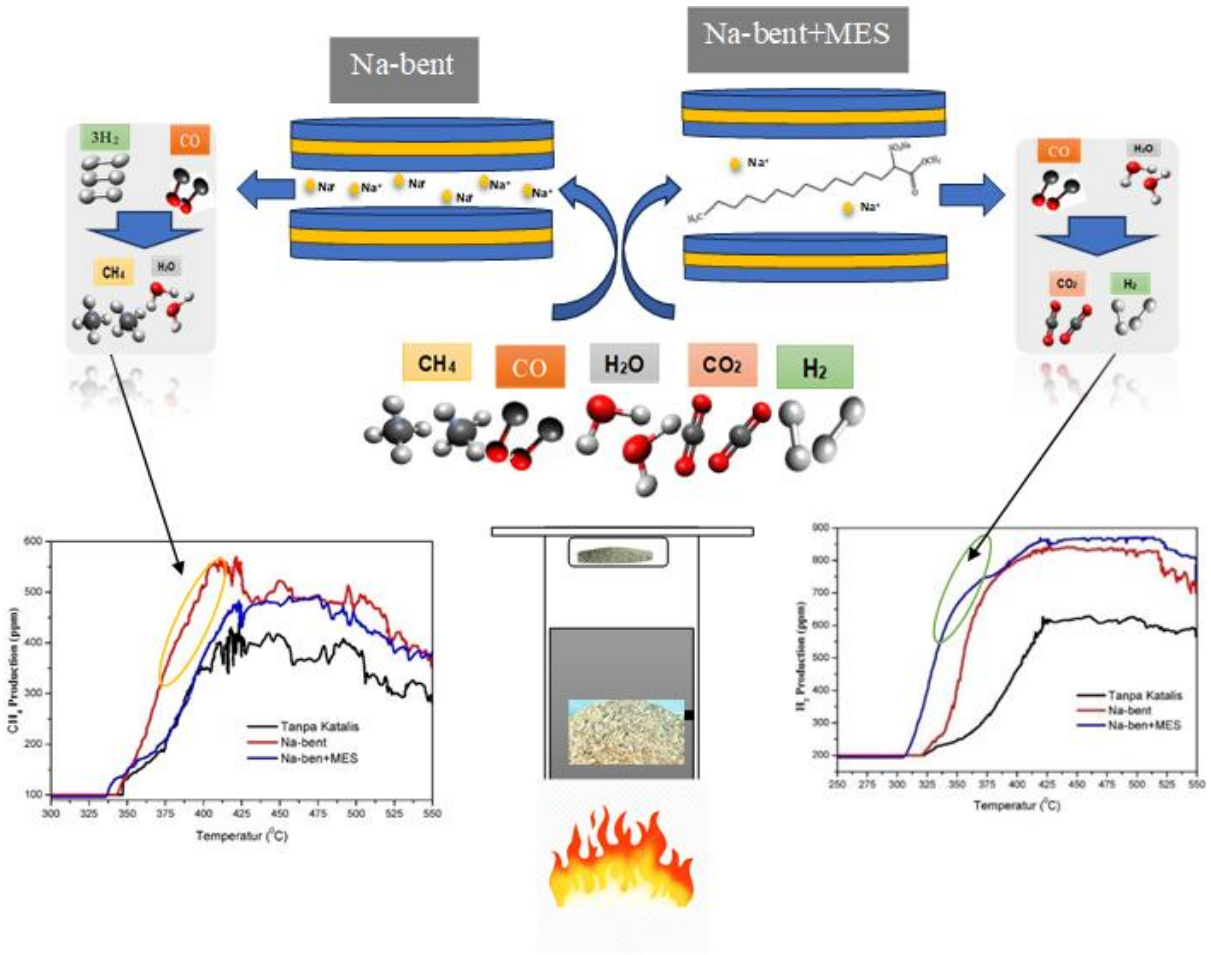

Figure 11. Impact of Na-bentonite modification using MES on the breakdown of molecules to generate methane and hydrogen gas.

4. CONCLUSION

Modification of Na-bentonite Catalyst using MES increases the activity and selectivity of the catalyst. The results of FTIR, XRD, UV-Vis, and SEM-EDX tests show changes in the characteristics of the Na-bentonite catalyst. Changes in the characteristics of Na-bentonite + MES, such as increased basal spacing distance, crystallinity, surface area, and the emergence of alkyl, ester, and sulfonate groups that increase the performance of the catalyst in producing hydrogen. The results of catalytic pyrolysis using Na-bentonite + MES catalysts produced hydrogen production reaching 876 ppm with an increase of 25.11%. This modification presents a potentially new method for creating environmentally friendly catalysts, which can be used to produce hydrogen more rapidly and at a lower cost.

5. ACKNOWLEDGMENT

We sincerely appreciate the financial support provided by the Center for Higher Education Funding (BPPT) by the Indonesian Education Scholarship (BPI), the Center for Higher Education Funding and Assessment (PPAPT), and the Indonesia Endowment Fund for Education Agency (LPDP) under the Ministry of Finance of the Republic of Indonesia for granting the scholarship and supporting this research.

DOI: https://doi.org/10.17509/ajse.v5i3.88898
p- ISSN 2776-6098 e- ISSN 2776-5938

6. AUTHORS' NOTE

The authors declare that there is no conflict of interest regarding the publication of this article. Authors confirmed that the paper was free of plagiarism.

7. REFERENCES

[1] Abedi, A., and Dalai, A. K. (2019). Steam gasification of oat hull pellets over Ni-based catalysts: Syngas yield and tar reduction. *Fuel*, *254*, 115585.

[2] Aprianti, N., Faizal, M., Said, M., and Nasir, S. (2021). Catalytic gasification of oil palm empty fruit bunch by using Indonesian bentonite as the catalyst. *Istrazivanja I Projektovanja Za Privredu*, *19*(2), 334–343.

[3] Setiabudi, H. D., Aziz, M. A. A., Abdullah, S., Teh, L. P., and Jusoh, R. (2020). Hydrogen production from catalytic steam reforming of biomass pyrolysis oil or bio-oil derivatives: A review. *International Journal of Hydrogen Energy*, *45*(36), 18376-18397.

[4] Wang, W., Ma, Y., Chen, G., Quan, C., Yanik, J., Gao, N., and Tu, X. (2022). Enhanced hydrogen production using a tandem biomass pyrolysis and plasma reforming process. *Fuel Processing Technology*, *234*, 107333.

[5] Suprianto, T., Wijayanti, W., and Wardana, I. N. G. (2021). Synergistic effect of curcumin and activated carbon catalyst enhancing hydrogen production from biomass pyrolysis. *International Journal of Hydrogen Energy*, *46*(10), 7147-7164.

[6] Li, Z., Tao, L., Yang, Q., Chen, L., Qi, H., Ma, X., and Ben, H. (2023). Mechanism research on hydrogen production from catalytic pyrolysis of waste tire rubber. *Fuel*, *331*, 125846.

[7] Wu, Q., Leng, S., Zhang, Q., and Xiao, J. (2021). Resource and environmental assessment of pyrolysis-based high-value utilization of waste passenger tires. *Waste Management*, *126*, 201-208.

[8] Li, W., Wei, M., Liu, Y., Ye, Y., Li, S., Yuan, W., and Wang, D. (2019). Catalysts evaluation for production of hydrogen gas and carbon nanotubes from the pyrolysis-catalysis of waste tyres. *International Journal of Hydrogen Energy*, *44*(36), 19563-19572.

[9] Sridevi, V., Surya, D. V., Reddy, B. R., Shah, M., Gautam, R., Kumar, T. H., and Basak, T. (2024). Challenges and opportunities in the production of sustainable hydrogen from lignocellulosic biomass using microwave-assisted pyrolysis: A review. *International Journal of Hydrogen Energy*, *52*, 507-531.

[10] Djimasbe, R., Ilyasov, I. R., Kwofie, M., Khelkhal, M. A., Emelianov, D. A., Al-Muntaser, A. A., and Varfolomeev, M. A. (2022). Direct hydrogen production from extra-heavy crude oil under supercritical water conditions using a catalytic (Ni-Co/Al2O3) upgrading process. *Catalysts*, *12*(10), 1183.

[11] Hamad, M. A., Radwan, A. M., Heggo, D. A., and Moustafa, T. (2016). Hydrogen rich gas production from catalytic gasification of biomass. *Renewable Energy*, *85*, 1290-1300.

[12] Ngo, T. N. L. T., Chiang, K. Y., Liu, C. F., Chang, Y. H., and Wan, H. P. (2021). Hydrogen production enhancement using hot gas cleaning system combined with prepared Ni-based catalyst in biomass gasification. *International Journal of Hydrogen Energy*, *46*(20), 11269-11283.

[13] Veses Roda, A., Aznar, M., López Sebastián, J. M., Callén Romero, M. S., Murillo Villuendas, R., and García Martínez, T. (2014). Production of upgraded bio-oils by

DOI: https://doi.org/10.17509/ajse.v5i3.88898
p- ISSN 2775-6793 e- ISSN 2775-6815

biomass catalytic pyrolysis in an auger reactor using low cost materials. *Fuel*, *141*, 17-22.

[14] Chong, C. C., Setiabudi, H. D., and Jalil, A. A. (2020). Dendritic fibrous SBA-15 supported nickel (Ni/DFSBA-15): A sustainable catalyst for hydrogen production. *International Journal of Hydrogen Energy*, *45*(36), 18533-18548.

[15] Das, T. K., and Poater, A. (2021). Review on the use of heavy metal deposits from water treatment waste towards catalytic chemical syntheses. *International Journal of Molecular Sciences*, *22*(24), 13383.

[16] Bangar, S. P., Ilyas, R. A., Chowdhury, A., Navaf, M., Sunooj, K. V., and Siroha, A. K. (2023). Bentonite clay as a nanofiller for food packaging applications. *Trends in Food Science & Technology*, *142*, 104242.

[17] Laksono, P. J., and Patriot, E. A. (2022). Analisis Blibiometrik Penelitian Jenis Lempung: Kontribusi Zeolit, Montmorilonoit, dan Bentonit. *Prosiding Seminar Nasional Sains Dan Teknologi Terapan*, *5*(2), 407–418.

[18] Jeenpadiphat, S., and Tungasmita, D. N. (2014). Esterification of oleic acid and high acid content palm oil over an acid-activated bentonite catalyst. *Applied Clay Science*, *87*, 272-277.

[19] Irawan, D., Wijayanti, W., Wahyudi, S., and Wardana, I. N. G. (2025). Modification effects of Na-bentonite catalyst with organic compounds increasing hydrogen production from biomass pyrolysis. *Case Studies in Chemical and Environmental Engineering*, *11*, 101206.

[20] Wang, L., and Wang, A. (2008). Adsorption properties of Congo Red from aqueous solution onto surfactant-modified montmorillonite. *Journal of Hazardous Materials*, *160*(1), 173-180.

[21] Charoentanaworakun, C., Srisuriyachai, F., Assabumrungrat, S., and Soottitantawat, A. (2023). Performance and salinity tolerance of palm oil-derived anionic biosurfactant and synthetic surfactant for waxy oil recovery in sandstone reservoirs. *Energy & Fuels*, *37*(17), 13191-13201.

[22] Zhou, J., and Sun, Q. (2022). Sodium alginate/modified bentonite composite bead adsorptive removal of norfloxacin: static and dynamic adsorption. *Polymers*, *14*(19), 3984.

[23] Thakur, S., Verma, A., Kumar, V., Yang, X. J., Krishnamurthy, S., Coulon, F., and Thakur, V. K. (2022). Cellulosic biomass-based sustainable hydrogels for wastewater remediation: chemistry and prospective. *Fuel*, *309*, 122114.

[24] Saeed, M., Farooq, K., Nafees, M., Arshad, M., Akhter, M. S., and Waseem, A. (2020). Green and eco-friendly removal of mycotoxins with organo-bentonites; isothermal, kinetic, and thermodynamic studies. *Clean–Soil, Air, Water*, *48*(9), 1900427.

[25] Lin, Z., Yang, Y., Liang, Z., Zeng, L., and Zhang, A. (2021). Preparation of chitosan/calcium alginate/bentonite composite hydrogel and its heavy metal ions adsorption properties. *Polymers*, *13*(11), 1891.

[26] Motawie, A. M., Madany, M. M., El-Dakrory, A. Z., Osman, H. M., Ismail, E. A., Badr, M. M., and Abulyazied, D. E. (2014). Physico-chemical characteristics of nano-organo bentonite prepared using different organo-modifiers. *Egyptian Journal of*

DOI: https://doi.org/10.17509/ajse.v5i3.88898
p- ISSN 2776-6098 e- ISSN 2776-5938

Petroleum, *23*(3), 331-338.

[27] Nousir, S., Arus, V. A., Shiao, T. C., Bouazizi, N., Roy, R., and Azzouz, A. (2019). Organically modified activated bentonites for the reversible capture of CO2. *Microporous and Mesoporous Materials*, *290*, 109652.

[28] Obradović, M., Daković, A., Smiljanić, D., Marković, M., Ožegović, M., Krstić, J., and Milojević-Rakić, M. (2023). Bentonite modified with surfactants—efficient adsorbents for the removal of non-steroidal anti-inflammatory drugs. *Processes*, *12*(1), 96.

[29] Yuliana, M., Sutrisno, R. J., Hermanto, S., Ismadji, S., Wijaya, C. J., Santoso, S. P., and Ju, Y. H. (2020). Hydrophobic cetyltrimethylammonium bromide-pillared bentonite as an effective palm oil bleaching agent. *ACS Omega*, *5*(44), 28844-28855.

[30] Garadimani, K. R., Raju, G. U., and Kodancha, K. G. (2015). Study on mechanical properties of corn cob particle and e-glass fiber reinforced hybrid polymer composites. *American Journal of Materials Science*, *5*(3C), 86-91.

[31] Bunaciu, A. A., UdriŞTioiu, E. G., and Aboul-Enein, H. Y. (2015). X-ray diffraction: instrumentation and applications. *Critical Reviews in Analytical Chemistry*, *45*(4), 289-299.

[32] Kar, Y., and Mert, B. A. (2024). Catalytic pyrolysis of lignite with clay catalyst activated with spent pickling liquor. *Asia-Pacific Journal of Chemical Engineering*, *19*(1), e2983.

[33] Li, M., Zhang, Y. S., Cheng, S., Qu, B., Li, A., Meng, F., and Ji, G. (2023). The impact of heating rate on the decomposition kinetics and product distribution of algal waste pyrolysis with in-situ weight measurement. *Chemical Engineering Journal*, *457*, 141368.

[34] Qin, Z., Yuan, P., Yang, S., Liu, D., He, H., and Zhu, J. (2014). Silylation of Al13-intercalated montmorillonite with trimethylchlorosilane and their adsorption for Orange II. *Applied Clay Science*, *99*, 229-236.

[35] Chauhan, T., Udayakumar, M., Shehab, M. A., Kristaly, F., Lesko, A. K., Ek, M., and Németh, Z. (2022). Synthesis, characterization, and challenges faced during the preparation of zirconium pillared clays. *Arabian Journal of Chemistry*, *15*(4), 103706.

[36] Mobarak, M., Selim, A. Q., Mohamed, E. A., and Seliem, M. K. (2018). A superior adsorbent of CTAB/H2O2 solution− modified organic carbon rich-clay for hexavalent chromium and methyl orange uptake from solutions. *Journal of Molecular Liquids*, *259*, 384-397.

[37] Abbou, B., Lebkiri, I., Ouaddari, H., El Amri, A., Achibat, F. E., Kadiri, L., and Rifi, E. H. (2023). Improved removal of methyl orange dye by adsorption using modified clay: combined experimental study using surface response methodology. *Inorganic Chemistry Communications*, *155*, 111127.

[38] Dongmo, L. M., Jiokeng, S. L., Pecheu, C. N., Walcarius, A., and Tonle, I. K. (2020). Amino-grafting of montmorillonite improved by acid activation and application to the electroanalysis of catechol. *Applied Clay Science*, *191*, 105602.

[39] Hakim, Y. M., Mohadi, R., and Royani, I. (2023). Ammonium-assisted intercalation of Java bentonite as effective of cationic dye removal. *Journal of Ecological Engineering*, *24*(2), 184-195.

DOI: https://doi.org/10.17509/ajse.v5i3.88898
p- ISSN 2775-6793 e- ISSN 2775-6815

[40] Abnisa, F. (2023). Enhanced liquid fuel production from pyrolysis of plastic waste mixtures using a natural mineral catalyst. *Energies*, *16*(3), 1224.

[41] Mamytbekov, G. K., Zheltov, D. A. E., and Nurtazin, Y. R. (2023). Synthesis and investigation of the properties of biphasic hybrid composites based on bentonite, copper hexacyanoferrate, acrylamide and acrylic acid hydrogel. *Polymers*, *15*(12), 2586.

[42] Rahman, M., Shuva, Z. M., Rahman, M. A., Ahmed, N., Sharmin, A., Laboni, A. A., and Saha, J. K. (2022). Catalytic pyrolysis of single-use waste polyethylene for the production of liquid hydrocarbon using modified bentonite catalyst. *European Journal of Inorganic Chemistry*, *2022*(34), e202200409.

[43] Antonelli, R., Martins, F. R., Malpass, G. R. P., da Silva, M. G. C., and Vieira, M. G. A. (2020). Ofloxacin adsorption by calcined Verde-lodo bentonite clay: Batch and fixed bed system evaluation. *Journal of Molecular Liquids*, *315*, 113718.

[44] Funes, I. G., Peralta, M. E., Pettinari, G. R., Carlos, L., and Parolo, M. E. (2020). Facile modification of montmorillonite by intercalation and grafting: The study of the binding mechanisms of a quaternary alkylammonium surfactant. *Applied Clay Science*, *195*, 105738.

[45] Alqahtani, M. D., Bin Jumah, M. N., Al-Hashimi, A., Allam, A. A., Abukhadra, M. R., and Bellucci, S. (2023). Synthesis and characterization of methoxy-exfoliated montmorillonite nanosheets as potential carriers of 5-fluorouracil drug with enhanced loading, release, and cytotoxicity properties. *Molecules*, *28*(15), 5895.

[46] Hernández-Giménez, A. M., de Kort, L. M., Whiting, G. T., Hernando, H., Puértolas, B., Pérez-Ramírez, J., and Weckhuysen, B. M. (2021). Upscaling effects on alkali metal-grafted ultrastable y zeolite extrudates for modeled catalytic deoxygenation of bio-oils. *ChemCatChem*, *13*(8), 1951-1965.

[47] Mao, J., Zhou, Y., Lv, G., and Zhou, R. (2022). Simultaneous detoxification of aflatoxin B1, zearalenone and deoxynivalenol by modified montmorillonites. *Molecules*, *27*(1), 315.

[48] Wang, G., Miao, Y., Sun, Z., and Zheng, S. (2018). Simultaneous adsorption of aflatoxin B1 and zearalenone by mono-and di-alkyl cationic surfactants modified montmorillonites. *Journal of Colloid and Interface Science*, *511*, 67-76.

[49] Guezzen, B., Ech-Chergui, A. N., Elaziouti, A., Demey, H., Zoukel, A., Didi, M. A., AND Adjdir, M. (2023). Adsorption isotherm and kinetic modeling of the Congo Red (CR) and Indigo Carmine (IC) dyes removal onto novel bentonite hybrid material. *ChemistrySelect*, *8*(25), e202300592.

[50] Denison, S. B., Jin, P., Dias Da Silva, P., Chu, C., Moorthy, B., Senftle, T. P., and Alvarez, P. J. (2023). Pyro-catalytic degradation of pyrene by bentonite-supported transition metals: Mechanistic insights and trade-offs with low pyrolysis temperature. *Environmental Science & Technology*, *57*(38), 14373-14383.

[51] Dwandaru, W. S. B., Fadli, A. L., Sari, E. K., and Isnaeni. (2020). Cdots and Cdots/S synthesis from nam-nam fruit (Cynometra cauliflora L.) via frying method using cooking oil. *Dig. J. Nanomaterial and Biostructure*, *15*(2), 555-560.

[52] Elfadly, A. M., Zeid, I. F., Yehia, F. Z., Abouelela, M. M., and Rabie, A. M. (2017). Production of aromatic hydrocarbons from catalytic pyrolysis of lignin over acid-

DOI: https://doi.org/10.17509/ajse.v5i3.88898
p- ISSN 2776-6098 e- ISSN 2776-5938

activated bentonite clay. *Fuel Processing Technology*, *163*, 1-7.

[53] Sari, E. K., Sekartaji, D., and Dwandaru, W. S. B. (2020). Nanomaterial Carbon-Dots berbahan dasar daun sirih (Piper Betle L.) sebagai antibakteri terhadap bakteri S. Mutans dan E. Coli. *Positron*, *10*(2), 105-112.

[54] Guo, D., Wan, Y., Li, J., Liu, R., Liu, L., and Xue, Q. (2023). Comparative assessment of modified bentonites as retardation barrier: adsorption performance and characterization. *Environmental Earth Sciences*, *82*(2), 58.

[55] RAK, H. N., Kristiantoro, T., Taryana, Y., Siswanto, E., and Wardana, I. N. G. (2024). Synthesis and characterization of Bamboo Activated Carbon (BAC) and Clitoria Ternatea Powder (CTP) for enhanced electromagnetic wave absorption. *Case Studies in Chemical and Environmental Engineering*, *10*, 100947.

[56] Sofi'i, Y. K., Siswanto, E., Ueda, T., and Wardana, I. N. G. (2020). The role of activated carbon in boosting the activity of clitoria ternatea powder photocatalyst for hydrogen production. *International Journal of Hydrogen Energy*, *45*(43), 22613-22628.

[57] García-García, F. A., Cristiani-Urbina, E., Morales-Barrera, L., Rodríguez-Peña, O. N., Hernández-Portilla, L. B., and Flores-Ortíz, C. M. (2023). Spectroscopic and microestructural evidence for T-2 toxin adsorption mechanism by natural bentonite modified with organic cations. *Toxins*, *15*(7), 470.

[58] Reis, C. A., Júnior, M. G., Moreira, F. K. V., Marconcini, J. M., and Vaz, L. E. V. D. S. B. (2023). Synthesis and characterization of chitosan/montmorillonite nanocomposites for application as edible coating. *Food Science and Technology International*, *29*(1), 25-39.

[59] Xu, Y., Su, T., Luo, X., Qin, Z., and Ji, H. (2023). Ni-Ti intercalated and supported bentonite for selective hydrogenation of cinnamaldehyde. *ChemPhysChem*, *24*(10), e202200703.

[60] Hassan, W. A., Ahmed, E. A., Moneim, M. A., Shaban, M. S., El-Sherbeeny, A. M., Siddiqui, N., and Abukhadra, M. R. (2021). Sulfonation of natural carbonaceous bentonite as a low-cost acidic catalyst for effective transesterification of used sunflower oil into diesel; statistical modeling and kinetic properties. *ACS Omega*, *6*(46), 31260-31271.

[61] Azizi, J., and Davarnejad, R. (2023). Electro-Fenton technique associated with core-shell Fe@ Fe2O3 nanoparticles-bentonite catalyst for pre-treating a super-pollutant industrial wastewater. *Journal of Water Process Engineering*, *51*, 103385.

[62] Hasanudin, H., Asri, W. R., Said, M., Hidayati, P. T., Purwaningrum, W., Novia, N., and Wijaya, K. (2022). Hydrocracking optimization of palm oil to bio-gasoline and bio-aviation fuels using molybdenum nitride-bentonite catalyst. *RSC Advances*, *12*(26), 16431-16443.

[63] Rodríguez-Castellón, E., Delgado, D., Dejoz, A., Vázquez, I., Agouram, S., Cecilia, J. A., and López Nieto, J. M. (2020). Enhanced NiO dispersion on a high surface area pillared heterostructure covered by niobium leads to optimal behaviour in the oxidative dehydrogenation of ethane. *Chemistry–A European Journal*, *26*(42), 9371-9381.

[64] Uebe, J., Kryzevicius, Z., Majauskiene, R., Dulevicius, M., Kosychova, L.,and& Zukauskaite, A. (2022). Use of polypropylene pyrolysis oil in alternative fuel production. *Waste Management & Research*, *40*(8), 1220-1230.

[65] Yang, C., Xu, H., Shi, J., Liu, Z., and Zhao, L. (2021). Preparation and photocatalysis of

DOI: https://doi.org/10.17509/ajse.v5i3.88898
p- ISSN 2775-6793 e- ISSN 2775-6815

CuO/bentonite based on adsorption and photocatalytic activity. *Materials*, *14*(19), 5803.

[66] Alavinia, S., Ghorbani-Vaghei, R., Ghiai, R., and Gharehkhani, A. (2023). Cu (ii) immobilized on poly (guanidine-sulfonamide)-functionalized Bentonite@ MgFe 2 O 4: a novel magnetic nanocatalyst for the synthesis of 1, 4-dihydropyrano [2, 3-c] pyrazole. *RSC Advances*, *13*(16), 10667-10680.

[67] Pan, Y., Zhang, X., Ji, C., Zhan, Q., Li, Z., Guan, J., and Huang, J. (2023). Modification method of high-efficiency organic bentonite for drilling fluids: a review. *Molecules*, *28*(23), 7866.

[68] Jeyakumar, N., Huang, Z., Balasubramanian, D., Le, A. T., Nguyen, X. P., Pandian, P. L., and Hoang, A. T. (2022). Experimental evaluation over the effects of natural antioxidants on oxidation stability of binary biodiesel blend. *International Journal of Energy Research*, *46*(14), 20437-20461.

[69] Palone, A., Casadevall, G., Ruiz-Barragan, S., Call, A., Osuna, S., Bietti, M., and Costas, M. (2023). C–H bonds as functional groups: simultaneous generation of multiple stereocenters by enantioselective hydroxylation at unactivated tertiary C–H bonds. *Journal of the American Chemical Society*, *145*(29), 15742-15753.

[70] Mohanty, U. S., Ali, M., Azhar, M. R., Al-Yaseri, A., Keshavarz, A., and Iglauer, S. (2021). Current advances in syngas (CO+ H2) production through bi-reforming of methane using various catalysts: A review. *International Journal of Hydrogen Energy*, *46*(65), 32809-32845.

DOI: https://doi.org/10.17509/ajse.v5i3.88898
p- ISSN 2776-6098 e- ISSN 2776-5938